

# Virtual Element Method for Second Order Elliptic Eigenvalue Problems

Francesca Gardini <sup>\*1</sup> and Giuseppe Vacca <sup>†2</sup>

<sup>1</sup>Dipartimento di Matematica “F. Casorati”, Università degli Studi di Pavia, via Ferrata 1, I-27100 Pavia, Italy

<sup>2</sup>Dipartimento di Matematica e Applicazioni, Università degli Studi di Milan-Bicocca, Via Roberto Cozzi, 55 - 20125 Milano, Italy

October 14, 2016

## Abstract

We introduce the Virtual Element Method (VEM) for elliptic eigenvalue problems. The main result of the paper states that VEM provides an optimal order approximation of the eigenmodes. A wide set of numerical tests confirm the theoretical analysis.

## 1 Introduction

The Virtual Element Method (VEM) is a brand new approximation technique introduced in [7] which has been applied to several problems. In its abstract formulation the method is a generalization of the conforming finite element method which allows, nevertheless, the use of general polygonal and polyhedral meshes without having to integrate complex non-polynomial functions on the elements.

The Virtual Element Method has been developed successfully for a large range of problems: the linear elasticity problems, both for the compressible and the nearly incompressible case [8, 35], a stream and a non-conforming formulation of VEMs for the Stokes problem [3, 30], the non-linear elastic and inelastic deformation problems, mainly focusing on a small deformation regime [16], the Darcy problem in mixed form [26], the plate bending problem [27], the Steklov eigenvalue problem [38], the general second order elliptic problems in primal [12] and mixed form [10], the Cahn-Hilliard equation [4], the Helmholtz problem [39], the discrete fracture network simulations [22, 21], the time-dependent diffusion problems [42, 41] and the Stokes problem [18]. In [5, 31] the authors present a non-conforming Virtual Element Space. *A posteriori* error estimates are studied in [20, 29, 37].  $H(\text{div})$  and  $H(\text{curl})$  VEM and VEM with arbitrary regularity are presented in [14] and [19], respectively. In [15] the VEM *hp* version is analyzed. Finally in [13, 11] the authors introduce the last version of Virtual Element spaces, the Serendipity VEM spaces that, in analogy with the Serendipity FEMs, allows to reduce the number of degrees of freedom.

In this paper we study the Virtual Element Method applied to elliptic eigenvalue problems. As a model problem we consider the Laplace eigenvalue problem. Nevertheless the analysis generalizes straightforward to the case of more general second order elliptic eigenvalue problems. The discretization of the problem requires the introduction of two discrete bilinear forms, one being the approximated grad-grad form and the other being a discrete version of the  $L^2$ -inner product. The latter one is built using the techniques of [2]. In particular, we consider both a non-stabilized form and a stabilized one, and we study the convergence properties of the corresponding discrete formulations. It is shown that the Virtual Element Method provides

---

<sup>\*</sup>francesca.gardini@unipv.it

<sup>†</sup>giuseppe.vacca@unimib.it

optimal convergence rates both for the eigenfunctions and the eigenvalues.

The paper is organized as follows. In Section 2, we set up the model eigenproblem, and in Section 3 we introduce the virtual element formulation of the problem. In Sections 4 we recall some fundamental results for the spectral approximation of compact operators. In Section 5 we prove the main results of the paper, which consist in the a priori error estimates for the eigenvalue problems. We discuss the implementation details in Section 6 and show the behaviour of the method for a set of numerical examples. We finally draw the conclusions in Section 7.

## 2 Setting of the problem

We are interested in the problem of computing the eigenvalues of the Laplace operator, namely

find  $\lambda \in \mathbb{R}$  such that there exists  $u$ , with  $\|u\|_0 = 1$  satisfying

$$\begin{cases} -\Delta u = \lambda u & \text{in } \Omega \\ u = 0 & \text{on } \Gamma, \end{cases} \quad (1)$$

where  $\Omega \subset \mathbb{R}^n$  ( $n = 2, 3$ ) is a bounded polygonal/polyhedral domain with Lipschitz boundary  $\Gamma$ .

For ease of exposition, we focus on the case of Dirichlet boundary conditions in the two-dimensional case. The three-dimensional case and the extension to other boundary conditions are analogous but more technical.

The variational formulation of problem (1) reads:

find  $\lambda \in \mathbb{R}$  such that there exists  $u \in V$ , with  $\|u\|_0 = 1$  satisfying

$$a(u, v) = \lambda b(u, v) \quad \forall v \in V, \quad (2)$$

where  $V = H_0^1(\Omega)$ ,  $a(u, v) = \int_{\Omega} \nabla u \cdot \nabla v$ , and  $b(\cdot, \cdot)$  denotes the  $L^2$ -inner product.

It is well-known that the eigenvalues of problem (2) form a positive increasing divergent sequence, and that the corresponding eigenfunctions are an orthonormal basis of  $V$  with respect both to the  $L^2$ -inner product and to the scalar product associated with the bilinear form  $a(\cdot, \cdot)$ .

Due to regularity results [1], there exists a constant  $r > 1/2$  depending on  $\Omega$ , such that the solution  $u$  belongs to the space  $H^{1+r}(\Omega)$ . It can be proved that  $r$  is at least one if  $\Omega$  is a convex domain, while  $r$  is at least  $\pi/\omega - \varepsilon$  for any  $\varepsilon > 0$  for a non-convex domain, being  $\omega < 2\pi$  the maximum interior angle of  $\Omega$ .

We will also need the source problem associated with the eigenvalue problem (2): given  $f \in L^2(\Omega)$ , find  $u^s \in V$  such that

$$a(u^s, v) = b(f, v) \quad \forall v \in V. \quad (3)$$

Throughout the paper, we will make use of the following notation. We will denote by  $|\cdot|_{s,\omega}$  and  $\|\cdot\|_{s,\omega}$  the seminorm and the norm in the Sobolev space  $H^s(\omega)$ , respectively, while  $(\cdot, \cdot)_{\omega}$  will denote the  $L^2$ -inner product over the domain  $\omega$ . Moreover, if  $\omega = \Omega$ , the subscript  $\omega$  may be omitted. For a positive integer  $k$ ,  $\mathbb{P}_k(\omega)$  will denote the space of polynomials on  $\omega$  of degree at most  $k$ . Finally,  $a^{\omega}(\cdot, \cdot)$  will denote the restriction of the form  $a(\cdot, \cdot)$  on  $\omega$ .

## 3 Virtual Element discretization

In this section, we briefly recall the Virtual Element discretization of the source problem (3) and its main properties (for further details, we refer to the original papers [7, 2]), and we state the VEM approximation of the eigenvalue problem (2).

Let  $\{\mathcal{T}_h\}_h$  be a sequence of decompositions of  $\Omega$  into polygons  $P$ , and let  $\mathcal{E}_h$  denote the set of edges  $e$  of  $\mathcal{T}_h$ . For every element  $P$ , we denote by  $|P|$  its area and by  $h_P$  its diameter. Similarly, for each edge  $e$ ,  $|e|$  will denote its length. Depending on the context,  $\partial P$  may denote the boundary of element  $P$  or the set of the element edges. As usual, the mesh size  $h$  is the maximum diameter of the elements  $P$  in  $\mathcal{T}_h$ .

In accordance with [7], we assume the following mesh regularity condition: there exist two positive constants  $\gamma$  and  $c$ , independent of  $h$ , such that each element  $P \in \mathcal{T}_h$  is star-shaped with respect to a ball of radius greater than  $\gamma h_P$ , and for each element  $P \in \mathcal{T}_h$  the distance between any two vertices of  $P$  is greater than  $ch_P$ .

Following [7, 2], for every integer  $k \geq 1$  and for every element  $P \in \mathcal{T}_h$  we define

$$\tilde{V}_h^k(P) := \{v \in C^0(\partial P) : v|_e \in \mathbb{P}_k(e) \ \forall e \subset \partial P, \Delta u \in \mathbb{P}_k(P)\}.$$

For each  $v$  in  $\tilde{V}_h^k(P)$ , the following set of degrees of freedom are unisolvent:

1. the values  $v(V_i)$  at the vertices  $V_i$  of  $P$ ,

and for  $k \geq 2$  the scaled edge and element moments up to order  $k - 2$

2.  $\frac{1}{|e|} \int_e v m \, ds, \quad \forall m \in \mathcal{M}_{k-2}(e)$ , on each edge  $e$  of  $P$ ,
3.  $\frac{1}{|P|} \int_P v m \, dx, \quad \forall m \in \mathcal{M}_{k-2}(P)$ ,

where  $\mathcal{M}_{k-2}(\omega)$  denotes the set of scaled monomials on  $\omega$

$$\mathcal{M}_{k-2}(\omega) = \left\{ \left( \frac{\mathbf{x} - \mathbf{x}_\omega}{h_\omega} \right)^{\mathbf{s}}, |\mathbf{s}| \leq k - 2 \right\}$$

being  $\mathbf{x}_\omega$  the barycenter of  $\omega$ .

*Remark 3.1.* The above degrees of freedom allows to exactly compute the  $L^2(P)$ -projection onto the space of piecewise polynomial of degrees at most  $k - 2$ . We observe that instead they are not enough to compute the projection onto the space of piecewise polynomial of degree  $k$ .

From the degrees of freedom, on each element  $P$  we can construct and exactly compute a projection operator  $\Pi_k^\nabla : \tilde{V}_h^k(P) \rightarrow \mathbb{P}_k(P)$  defined as follows:

$$a^P(\Pi_k^\nabla v - v, p) = 0 \quad \forall p \in \mathbb{P}_k(P) \quad (4)$$

and

$$\int_{\partial P} (\Pi_k^\nabla v - v) ds = 0 \quad \text{for } k = 1 \quad (5)$$

or

$$\int_P (\Pi_k^\nabla v - v) dx = 0 \quad \text{for } k \geq 2. \quad (6)$$

We observe that this operator is well-defined also for functions in  $H^1(P)$ , but in this case it is not exactly computable. On the other hand, for all  $v \in \tilde{V}_h^k$ ,  $\Pi_k^\nabla v$  can be computed only in terms of the degrees of freedom of  $v$ .

The local virtual space is then defined as

$$V_h^k(P) = \left\{ v \in \tilde{V}_h^k(P) : \int_P v p \, dx = \int_P (\Pi_k^\nabla v) p \, dx \ \forall p \in (\mathbb{P}_k / \mathbb{P}_{k-2}(P)) \right\}, \quad (7)$$

where  $(\mathbb{P}_k / \mathbb{P}_{k-2}(P))$  denotes the space of polynomials in  $\mathbb{P}_k(P)$   $L^2$ -orthogonal to all polynomials in  $\mathbb{P}_{k-2}(P)$ .

We recall that, by construction, the local space  $V_h^k(P)$  enjoys the following fundamental properties (see [2]):

1. the space  $\mathbb{P}_k(P) \subset V_h^k(P)$ . This property will guarantee the optimal order of approximation
2. the set of degrees of freedom of the local space  $\tilde{V}_h^k(P)$  are unisolvent also for the space  $V_h^k(P)$

3. since  $V_h^k(P) \subset \tilde{V}_h^k(P)$ , the operator  $\Pi_k^\nabla$  is well-defined on  $V_h^k(P)$  and it is still computable in terms of the degrees of freedom
4. the standard  $L^2$ -projection operator  $\Pi_k^0 : V_h^k(P) \rightarrow \mathbb{P}_k(P)$  is computable only in terms of the degrees of freedom
5. for all  $v \in V_h^k(P)$  the vectorvalued function  $\Pi_{k-1}^0 \nabla v_h$  can be explicitly computed from the degrees of freedom, see [12].

The global discrete space is hence defined in the finite element way as

$$V_h^k = \{v \in V : v|_P \in V_h^k(P) \quad \forall P \in \mathcal{T}_h\},$$

and the Virtual Element discretization of source problem (3) reads

$$\begin{cases} \text{find } u_h^s \in V_h^k \text{ such that} \\ a_h(u_h^s, v_h) = \langle f_h, v_h \rangle \quad \forall v_h \in V_h^k, \end{cases} \quad (8)$$

where  $\langle \cdot, \cdot \rangle$  denotes the duality pairing in  $V_h^k$ , and  $f_h \in (V_h^k)'$ . In particular,

$$\langle f_h, v_h \rangle = \sum_{P \in \mathcal{T}_h} (\Pi_k^0 f, v_h)_P.$$

The discrete bilinear form  $a_h(\cdot, \cdot)$  splits as

$$a_h(u_h, v_h) = \sum_{P \in \mathcal{T}_h} a_h^P(u_h, v_h). \quad (9)$$

with

$$a_h^P(u_h, v_h) = a^P(\Pi_k^\nabla u_h, \Pi_k^\nabla v_h) + \sigma_P S^P((I - \Pi_k^\nabla)u_h, (I - \Pi_k^\nabla)v_h). \quad (10)$$

where  $S^P(\cdot, \cdot)$  denotes any symmetric positive definite bilinear form on the element  $P$  such that there exist two positive constants  $c_0$  and  $c_1$  such that

$$c_0 a^P(v, v) \leq S^P(v, v) \leq c_1 a(v, v) \quad \forall v \in V_h^k(P) \text{ with } \Pi_k^\nabla v = 0,$$

and  $\sigma_P > 0$  is a stabilization parameter independent of the element size [17].

The choice of the discrete form  $a_h(\cdot, \cdot)$  is driven by the need to satisfy the *k-consistency* and *stability* properties, i.e.

- *k-consistency*: for all  $v \in V_h^k$  and for all  $p \in \mathbb{P}_k(P)$  it holds

$$a_h^P(v, p) = a^P(v, p)$$

- *stability*: there exists two positive constants  $\alpha_*$ ,  $\alpha^*$ , independent of  $h$  and of  $P$ , such that

$$\alpha_* a^P(v, v) \leq a_h^P(v, v) \leq \alpha^* a^P(v, v) \quad \forall v \in V_h^k.$$

In particular, the first term in (10) ensures *k-consistency*, while the second one *stability*.

In [2] it has been proved that the discrete problem (8) is well-posed and that, for a suitable choice of the discrete load term  $f_h$ , the following optimal *a priori* error estimate holds.

**Theorem 3.1.** *Let  $u$  be the solution of problem (3) and  $u_h \in V_h^k$  be the solution of the discrete problem (8) with  $f_h = \Pi_k^0 f$ . If the right-hand side  $f$  is smooth enough, namely  $f \in H^{k-1}(\Omega)$ , and the exact solution  $u \in H^{k+1}(\Omega)$ , then*

$$\|u - u_h\|_1 \leq Ch^k |u|_{k+1}. \quad (11)$$

*Remark 3.2.* We observe that the same result holds also for general linear second order elliptic problems, provided the form  $a(\cdot, \cdot)$  is choosen as in (25). We refer to [12] for an exhaustive analysis.

Moreover, the following approximation and interpolation properties hold [28, 25].

**Theorem 3.2.** *There exists a constant  $C$ , depending only on  $k$  and  $\gamma$ , such that for every  $s$  with  $2 \leq s \leq k+1$ , for every  $h$ , for all  $P \in \mathcal{T}_h$ , and for every  $w \in H^s(\Omega)$  there exists a  $w_I \in V_h$  such that*

$$\|w - w_I\|_{0,P} + h_P |w - w_I|_{1,P} \leq Ch_P^s |w|_{s,P}. \quad (12)$$

**Theorem 3.3.** *There exists a constant  $C$ , depending only on  $k$  and  $\gamma$ , such that for every  $s$  with  $1 \leq s \leq k+1$  and for every  $w \in H^s(\Omega)$  there exists a  $w_\pi \in \mathbb{P}_k$  such that*

$$\|w - w_\pi\|_{0,P} + h_P |w - w_\pi|_{1,P} \leq Ch_P^s |w|_{s,P}. \quad (13)$$

We are now ready to write the VEM approximation of problem (2): find  $\lambda_h \in \mathbb{R}$  such that there exists  $u_h \in V_h^k$ , with  $\|u\|_0 = 1$  satisfying

$$a_h(u_h, v_h) = \lambda_h b_h(u_h, v_h) \quad \forall v_h \in V_h^k, \quad (14)$$

where  $b_h(\cdot, \cdot) = \sum_{P \in \mathcal{T}_h} b_h^P(\cdot, \cdot)$  is a symmetric bilinear forms defined on  $V_h^k \times V_h^k$ . Two possible choices for the discrete form  $b_h(\cdot, \cdot)$  are available. The first one is inspired by the virtual approximation of the load term in the source problem (8) and reads as follows:

$$b_h^P(u_h, v_h) = \int_P \Pi_k^0 u_h \Pi_k^0 v_h. \quad (15)$$

The second possible choice consists in considering a discrete bilinear form  $\tilde{b}_h(\cdot, \cdot)$  which enjoys not only the  $k$ -consistency property, but also the *stability* one. In this case, as done for the discrete form  $a_h(\cdot, \cdot)$ , we define

$$\tilde{b}_h^P(u_h, v_h) = \int_P \Pi_k^0 u_h \Pi_k^0 v_h + \tau_P h_P^2 \tilde{S}^P \left( (I - \Pi_k^0) u_h, (I - \Pi_k^0) v_h \right), \quad (16)$$

where  $\tilde{S}^P$  is any positive defined bilinear form on the element  $P$  such that there exist two positive constants  $\tilde{c}_0$  and  $\tilde{c}^1$  such that

$$\tilde{c}_0 b^P(v, v) \leq \tilde{S}^P(v, v) \leq \tilde{c}^1 b(v, v) \quad \forall v \in V_h^k(P) \text{ with } \Pi_k^0 v = 0,$$

and  $\tau^P > 0$  is a stabilization parameter independent of the element size.

*Remark 3.3.* In the definition of the discrete bilinear forms  $b_h(\cdot, \cdot)$  and  $\tilde{b}_h(\cdot, \cdot)$ , we project onto the space  $\mathbb{P}_k$  since it has been numerically observed that this gives more accurate results. For sure, this choice does not provide a better convergence rate, due to the  $k$ -consistency property.

*Remark 3.4.* Observe that the second power of  $h$  in front of the stabilizing term comes from a scaling argument.

The second VEM approximation of problem (2) then reads as find  $\tilde{\lambda}_h \in \mathbb{R}$  such that there exists  $\tilde{u}_h \in V_h^k$ , with  $\|\tilde{u}\|_0 = 1$  satisfying

$$a_h(\tilde{u}_h, v_h) = \tilde{\lambda}_h \tilde{b}_h(\tilde{u}_h, v_h) \quad \forall v_h \in V_h^k. \quad (17)$$

In what follows, we will also need the discrete source problem corresponding to the second discrete formulation (17), which reads as:

$$\begin{cases} \text{find } \tilde{u}_h^s \in V_h^k \text{ such that :} \\ a_h(\tilde{u}_h^s, v_h) = \tilde{b}_h(f, v_h) \quad \forall v_h \in V_h^k. \end{cases} \quad (18)$$

The well-posedness of the discrete formulation (18) steams from that of the discrete formulation (8), since the bilinear form  $a_h(\cdot, \cdot)$  is coercive (due to the *stability* property).

Summarizing, we consider two different discrete approximation of problems (2) and (3), with at the right hand side a non-stabilized bilinear form and a stablized one, respectively.

## 4 Spectral approximation for compact operators

In this section, we briefly recall some spectral approximation results that can be deduced from [6, 23, 36]. For more general results, we refer to the original papers.

Before stating the spectral approximation results, we introduce a natural compact operator associated with problem (2) and its discrete counterpart and we recall their connection with the eigenmode convergence.

Let  $T \in \mathcal{L}(L^2(\Omega))$  be the solution operator associated with problem (2), namely  $T : L^2(\Omega) \rightarrow L^2(\Omega)$  is defined by

$$\begin{cases} Tf \in V \text{ such that} \\ a(Tf, v) = b(f, v) \quad \forall v \in L^2(\Omega). \end{cases}$$

Operator  $T$  is self-adjoint and positive definite. Moreover, operator  $T$  is also compact due to the compact embedding of  $H^1(\Omega)$  into  $L^2(\Omega)$ .

Similarly, let  $T_h \in \mathcal{L}(L^2(\Omega))$  be the discrete solution operator associated with problem (8) defined as

$$\begin{cases} T_h f \in V \text{ such that} \\ a_h(T_h f, v_h) = b_h(f_h, v_h) \quad \forall v_h \in V_h^k. \end{cases}$$

Analogously, the discrete solution operator  $\tilde{T}_h \in \mathcal{L}(L^2(\Omega))$  associated with problem (18) is defined as

$$\begin{cases} \tilde{T}_h f \in V \text{ such that} \\ a_h(\tilde{T}_h f, v_h) = \tilde{b}_h(f, v_h) \quad \forall v_h \in V_h^k. \end{cases}$$

Operators  $T_h$  and  $\tilde{T}_h$  are self-adjoint and compact since their ranges are finite dimensional. Finally, the eigensolutions of the continuous and the discrete problems (2) and (14) are respectively related to the eigenmodes of operators  $T$  and  $T_h$  in the sense that the corresponding eigenvalues are inverse of each other and their eigenspaces coincide. By virtue of this correspondence, the convergence analysis can be derived from the spectral approximation theory for compact operators.

Since similar considerations hold for the eigenmodes of operators  $T$  and  $\tilde{T}_h$ , in the following we present only the results relative to operators  $T$  and  $T_h$ .

A sufficient condition for the correct spectral approximation of a compact operator  $T$  is the uniform convergence to  $T$  of the family of discrete operators  $\{T_h\}_h$  [6, 23]:

$$\|T - T_h\|_{\mathcal{L}(L^2(\Omega))} \rightarrow 0, \quad \text{as } h \rightarrow 0, \quad (19)$$

or, equivalently,

$$\|Tf - T_h f\|_0 \leq C\rho(h)\|f\|_0 \quad \forall f \in L^2(\Omega), \quad (20)$$

with  $\rho(h)$  tending to zero as  $h$  goes to zero.

We remark that (19), besides the convergence of the eigenmodes, contains also the information that no spurious eigenvalues pollute the spectrum. In fact,

- (i) each continuous eigenvalue is approximated by a number of discrete eigenvalues (counted with their multiplicity) that corresponds exactly to its multiplicity;
- (ii) each discrete eigenvalue approximates a continuous eigenvalue.

Since operator  $T$  is compact and self-adjoint, condition (19) is also necessary for the correct spectral approximation; see [24]. Regarding the rate of convergence of eigenvalues and eigenvectors, we refer to [6, (Theorem 11.1 and 11.2)].

A simple way to estimate the norm of the difference  $T - T_h$  is to use *a priori* error estimates.

## 5 Convergence analysis of the method

In this section we study the convergence of the discrete eigenmodes provided by the VEM approximation to the continuous ones. We will consider the non-stabilized discrete formulation (14) and the stabilized one (17) separately.

## 5.1 Convergence analysis for the first formulation

In the case of the first VEM approximation of problem (2), which corresponds to the choice of a non-stabilized  $b_h(\cdot, \cdot)$  form, the uniform convergence of the sequence of operators  $T_h$  to  $T$  directly stems from the *a priori* error estimates in Theorem 3.1. The optimal rate of convergence of the eigenfunctions and the double rate of convergence of the eigenvalues can then be deduced in a usual way from the classical results of spectral approximation for compact operators in variational form, see Theorems 11.1 and 11.2 in [6].

The following theorem ensures the convergence of eigenmodes.

**Theorem 5.1.** *The family of operators  $T_h$  associated with problem (8) converges uniformly to the operator  $T$  associated with problem (3), that is,*

$$\|T - T_h\|_{\mathcal{L}(L^2(\Omega))} \rightarrow 0 \text{ for } h \rightarrow 0.$$

Let  $\lambda$  be an eigenvalue of problem (2), with multiplicity  $m$ , and denote the corresponding eigenspace by  $\mathcal{E}_\lambda$ . Then exactly  $m$  discrete eigenvalues  $\lambda_{1,h}, \dots, \lambda_{m,h}$ , which are repeated according to their respective multiplicities, converge to  $\lambda$ . Moreover, let  $\mathcal{E}_{\lambda,h}$  be the direct sum of the eigenspaces corresponding to the eigenvalues  $\lambda_{1,h}, \dots, \lambda_{m,h}$ . Then, there exists a positive number  $h_0$  such that for  $h \leq h_0$  the following inequalities are true:

$$\begin{aligned} |\lambda - \lambda_{i,h}| &\leq Ch^{2t} \quad \forall i = 1, \dots, m, \\ \hat{\delta}(\mathcal{E}_\lambda, \mathcal{E}_{\lambda,h}) &\leq Ch^t, \end{aligned}$$

where the non-negative constant  $C$  is independent of  $h$ ,  $t = \min\{k, r\}$ , being  $k$  the order of the method and  $r$  the regularity index of the eigenfunction, and  $\hat{\delta}(\mathcal{E}_\lambda, \mathcal{E}_{\lambda,h})$  denotes the gap between  $\mathcal{E}_\lambda$  and  $\mathcal{E}_{\lambda,h}$ .

## 5.2 Convergence analysis for the second formulation

The convergence analysis of the second discrete formulation of problem (2), corresponding to the choice of the stabilized form  $\tilde{b}_h(\cdot, \cdot)$ , is more involved. In this case, we resort to the abstract theory of the spectral approximation for non-compact operators by Descloux, Nassif, and Rappaz (see [33, 34]).

We recall the main convergence theorem stated in [34].

**Theorem 5.2.** *Assume that the following two conditions are satisfied:*

$$\textbf{(P1): } \|(T - \tilde{T}_h)|_{V_h^k}\|_{\mathcal{L}(L^2(\Omega))} \rightarrow 0 \quad \textbf{(P2): } \lim_{h \rightarrow 0} \inf_{v_h \in V_h^k} \|v - v_h\|_V = 0 \quad \forall v \in V. \quad (21)$$

Then the eigenmodes convergence holds.

*Proof.* Property **(P2)** directly stems from the approximation properties of the virtual element space (Theorem 3.2). On the other hand, property **P1** can be proved as follows.

$$\|(T - \tilde{T}_h)|_{V_h^k}\|_{\mathcal{L}(L^2(\Omega))} \leq \|(T - T_h)|_{V_h^k}\|_{\mathcal{L}(L^2(\Omega))} + \|(T_h - \tilde{T}_h)|_{V_h^k}\|_{\mathcal{L}(L^2(\Omega))}.$$

By Theorem (5.1), the first terms goes to zero. We are left to prove that the second term goes to zero as well. To this end, we proceed as follows:

$$\|(T_h - \tilde{T}_h)|_{V_h^k}\|_{\mathcal{L}(L^2(\Omega))} = \sup_{g_h \in V_h^k} \frac{\|T_h g_h - \tilde{T}_h g_h\|_0}{\|g_h\|_0} = \sup_{g_h \in V_h^k} \frac{\|u_h^s - \tilde{u}_h^s\|_0}{\|g_h\|_0},$$

where  $u_h^s$  and  $\tilde{u}_h^s$  denote, respectively, the solutions of the discrete source problems (8) and (18) corresponding to  $g_h$ .

Let  $\delta_h = u_h^s - \tilde{u}_h^s$ . By the coercivness of the form  $a(\cdot, \cdot)$ , the stability of the form  $a_h(\cdot, \cdot)$ , the

discrete source problems (8) and (18), and the stability of the projection operator  $\Pi_P^0$ , it holds

$$\begin{aligned}\|\delta_h\|_0^2 &\leq Ca(\delta_h, \delta_h) \leq C \sum_{P \in \mathcal{T}_h} a_h^P(\delta_h, \delta_h) \\ &= -C \sum_{P \in \mathcal{T}_h} h_P^2 \tilde{S}^P \left( g_h - \Pi_k^0 g_h, \delta_h - \Pi_k^0 \delta_h \right) \\ &\leq Ch^2 \|g_h\|_0 \|\delta_h\|_0.\end{aligned}$$

The uniform convergence **(P2)** can also be proved with a duality argument. Following the lines of the proof of Theorem 3 in [2] we assume that  $\Omega$  is convex and denote by  $\phi \in H^2(\Omega)$  the solution of the dual problem:

$$a(v, \phi) = b(\delta_h, v) \quad \forall v \in V. \quad (22)$$

Then it holds

$$\|\phi\|_2 \leq C \|\delta_h\|_0. \quad (23)$$

Let  $\phi_I \in V_h^k$  as in Theorem 3.3. Then

$$\begin{aligned}\|\delta_h\|_0^2 &= a(\delta_h, \phi - \phi_I) + a(u_h^s, \phi_I) - a(\tilde{u}_h^s, \phi_I) \\ &= a(\delta_h, \phi - \phi_I) + a(u_h^s, \phi_I) - a_h(u_h^s, \phi_I) \\ &\quad + a_h(\tilde{u}_h^s, \phi_I) - a(\tilde{u}_h^s, \phi_I) \\ &\quad + a_h(u_h^s, \phi_I) - a_h(\tilde{u}_h^s, \phi_I) \\ &= I + II + III + IV.\end{aligned}$$

The first term can be easily estimated using the continuity of the form  $a(\cdot, \cdot)$ , Theorem 3.3, and the stability of the discrete problems (8) and (18):

$$a(\delta_h, \phi - \phi_I) \leq Ch \|g_h\|_0 \|\delta_h\|_0.$$

We estimate II in this way

$$\begin{aligned}a(u_h^s, \phi_I) - a_h(u_h^s, \phi_I) &= \sum_{P \in \mathcal{T}_h} \left( a^P(u_h^s - \Pi_k^0 u^s, \phi_I) - a_h^P(u_h^s - \Pi_k^0 u^s, \phi_I) \right) \\ &= \sum_{P \in \mathcal{T}_h} \left( a^P(u_h^s - \Pi_k^0 u^s, \phi_I - \Pi_1^0 \phi) - a_h^P(u_h^s - \Pi_k^0 u^s, \phi_I - \Pi_1^0 \phi) \right), \\ &\leq C \left( \|u_h^s - u^s\|_1 + \|u^s - \Pi_k^0 u^s\|_1 \right) \|\phi_I - \Pi_1^0 \phi\|_1\end{aligned}$$

where  $u^s$  denote the solution of problem (3) corresponding to  $g_h$  and we have used twice the *consistency* assumption. In [2] it has been proved that

$$\|\phi_I - \Pi_1^0 \phi\|_0 \leq Ch \|\delta_h\|_0,$$

thus, using the stability of the continuous and discrete source problems (3) and (8), we obtain

$$II \leq Ch \|g_h\|_0 \|\delta_h\|_0.$$

The fourth term can be estimated in a similar way as II.

Eventually, we estimate IV as follows:

$$\begin{aligned}a_h(u_h^s, \phi_I) - a_h(\tilde{u}_h^s, \phi_I) &= b_h(g_h, \phi_I) - \tilde{b}_h(g_h, \phi_I) \\ &= - \sum_{P \in \mathcal{T}_h} \tau_P h_P^2 \tilde{S}^P (g_h - \Pi_k^0 g_h, \phi_I - \Pi_k^0 \phi_I) \\ &\leq Ch^2 \|g_h\|_0 \|\delta_h\|_0.\end{aligned}$$

□

We end this section stating the convergence theorem for the second discrete approximation of problem (2).

**Theorem 5.3.** *The family of operators  $\tilde{T}_h$  associated with problem (18) converges uniformly to the operator  $T$  associated with problem (3), that is,*

$$\|T - \tilde{T}_h\|_{\mathcal{L}(L^2(\Omega))} \rightarrow 0 \text{ for } h \rightarrow 0.$$



Let  $\lambda$  be an eigenvalue of problem (2), with multiplicity  $m$ , and denote the corresponding eigenspace by  $\mathcal{E}_\lambda$ . Then exactly  $m$  discrete eigenvalues  $\tilde{\lambda}_{1,h}, \dots, \tilde{\lambda}_{m,h}$ , which are repeated according to their respective multiplicities, converge to  $\tilde{\lambda}$ . Moreover, let  $\mathcal{E}_{\tilde{\lambda},h}$  be the direct sum of the eigenspaces corresponding to the eigenvalues  $\tilde{\lambda}_{1,h}, \dots, \tilde{\lambda}_{m,h}$ . Then, there exists a positive number  $h_0$  such that for  $h \leq h_0$  the following inequalities are true:

$$\begin{aligned} |\tilde{\lambda} - \tilde{\lambda}_{i,h}| &\leq Ch^{2t} \quad \forall i = 1, \dots, m, \\ \hat{\delta}(\mathcal{E}_{\tilde{\lambda}}, \mathcal{E}_{\tilde{\lambda},h}) &\leq Ch^t, \end{aligned}$$

where the non-negative constant  $C$  is independent of  $h$ ,  $t = \min\{k, r\}$ , being  $k$  the order of the method and  $r$  the regularity index of the eigenfunction, and  $\hat{\delta}(\mathcal{E}_{\tilde{\lambda}}, \mathcal{E}_{\tilde{\lambda},h})$  denotes the gap between  $\mathcal{E}_{\tilde{\lambda}}$  and  $\mathcal{E}_{\tilde{\lambda},h}$ .

## 6 Numerical tests

In this section we present four numerical experiments to test the actual performance of the method, in particular we confirm the a priori bounds on the error of the eigenvalue approximation provided by Theorem 5.1 and Theorem 5.3. We consider the error quantities:

$$\epsilon_{h,\lambda} := |\lambda - \lambda_h|. \quad (24)$$

We briefly sketch an example of the construction of the stabilizing bilinear form  $S^P(\cdot, \cdot)$  and the selection of the stabilization parameter  $\sigma_P$  in (10) (resp.  $\tilde{S}^P(\cdot, \cdot)$  and  $\tau_P$  in (16)), that follows a standard VEM technique (cf. [7, 9] for more details). Let us denote with  $\bar{\mathbf{v}}_h, \bar{\mathbf{w}}_h \in \mathbb{R}^{N_P}$  the vectors containing the values of the  $N_P$  local degrees of freedom associated to  $v_h, w_h \in V_h^k(P)$ . Then, we set

$$S^P(v_h, w_h) = \tilde{S}^P(v_h, w_h) := \bar{\mathbf{v}}_h^T \bar{\mathbf{w}}_h.$$

For what concerns the stabilization parameters in the numerical tests we have chosen  $\sigma_P$  as the mean value of the eigenvalues of the matrix stemming from the consistency term  $a_h^P(\Pi_k^\nabla v_h, \Pi_k^\nabla w_h)$  for the grad-grad form (see (10)). In the same way we have picked  $\tau_P$  as the mean value of the eigenvalues of the matrix resulting from the term  $\frac{1}{h^2} \int_P \Pi_k^0 v_h \Pi_k^0 w_h$  for the mass matrix (see (16)).

*Test 6.1.* In the first test we consider the standard eigenvalue problem with homogeneous Dirichlet boundary conditions.

Regarding the computational domain, in the test we take the square domain  $\Omega = [0, 1]^2$ , which is partitioned using the following sequences of polygonal meshes:

- $\{\mathcal{V}_h\}_h$ : sequence of Voronoi meshes with  $h = 1/8, 1/16, 1/32, 1/64$ ,
- $\{\mathcal{T}_h\}_h$ : sequence of triangular meshes with  $h = 1/4, 1/8, 1/16, 1/32$ ,
- $\{\mathcal{Q}_h\}_h$ : sequence of square meshes with  $h = 1/8, 1/16, 1/32, 1/64$ .
- $\{\mathcal{W}_h\}_h$ : sequence of WEB-like meshes with  $h = 1/8, 1/16, 1/32, 1/64$ .

An example of the adopted meshes is shown in Figure 1. For the generation of the Voronoi meshes we used the code Polymesher [40]. The WEB-like meshes are composed by hexagons, generated starting from the triangular meshes  $\{\mathcal{T}_h\}_h$  and randomly displacing the midpoint of each (non boundary) edge.

It is well known that the eigenvalues of the problem are given by

$$\lambda = \pi^2(n^2 + m^2) \quad \text{for } n, m \neq 0.$$

We consider the VEM approximation problem (17) stemming from the stabilized bilinear form  $\tilde{b}_h(\cdot, \cdot)$ . We consider the polynomial degree of accuracy  $k = 1, 2, 3$  and we study the convergence of the errors  $\epsilon_{h,\lambda}$  with respect to  $h$  for the first six eigenvalues.

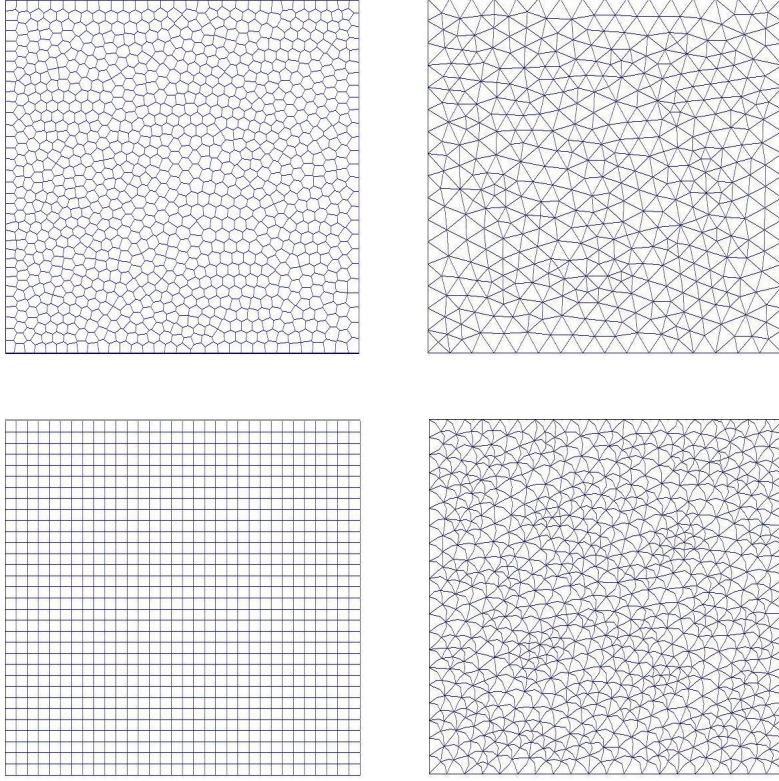


Figure 1: Test 1. Example of polygonal meshes:  $\mathcal{V}_{1/32}$ ,  $\mathcal{T}_{1/16}$ ,  $\mathcal{Q}_{1/32}$ ,  $\mathcal{W}_{1/32}$ .

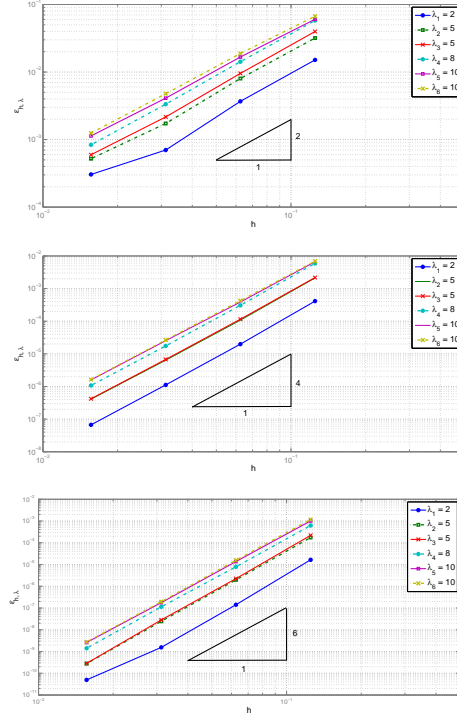


Figure 2: Test 1. Convergence plot for the eigenvalues for the sequence of meshes  $\mathcal{V}_h$  with  $k = 1, 2, 3$ .

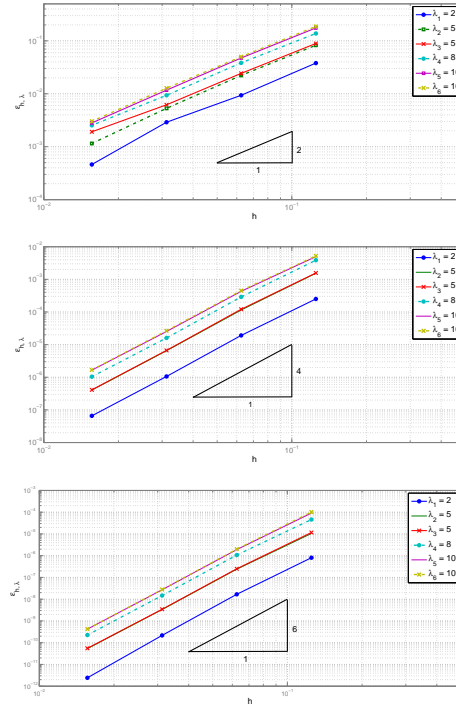


Figure 3: Test 1. Convergence plot for the eigenvalues for the sequence of meshes  $\mathcal{T}_h$  with  $k = 1, 2, 3$ .

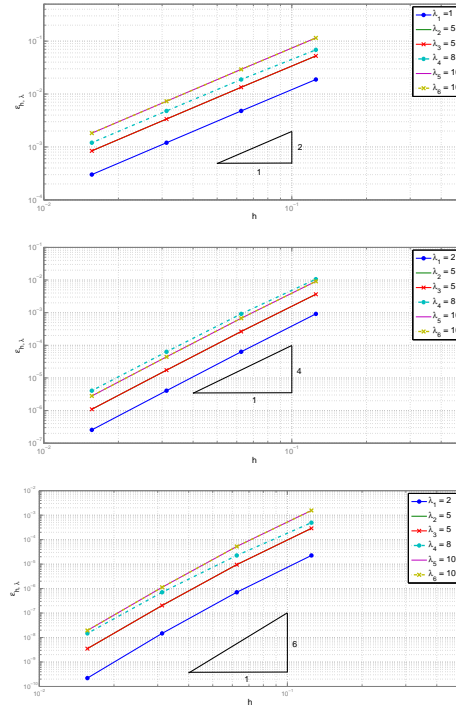


Figure 4: Test 1. Convergence plot for the eigenvalues for the sequence of meshes  $\mathcal{Q}_h$  with  $k = 1, 2, 3$ .

In Figure 2 we display the results for the sequence of Voronoi meshes  $\mathcal{V}_h$ . In Figure 3 we show the results for the sequence of meshes  $\mathcal{T}_h$ , while in Figure 4 we plot the results for the

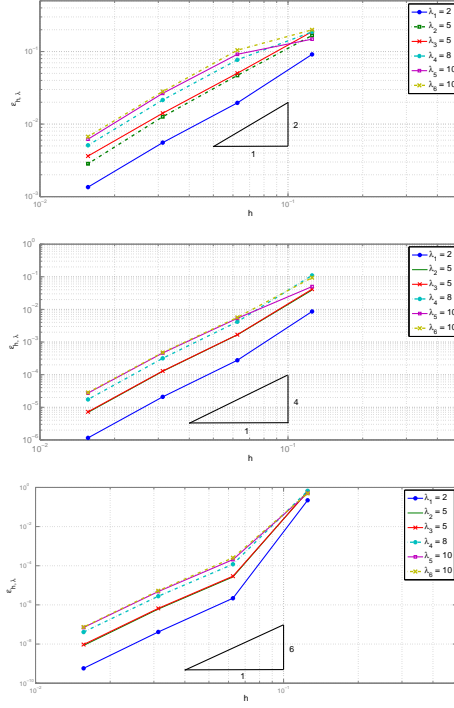


Figure 5: Test 1. Convergence plot for the eigenvalues for the sequence of meshes  $\mathcal{W}_h$  with  $k = 1, 2, 3$ .

sequence of meshes  $\mathcal{Q}_h$ , finally in 5 we exhibit the results for the sequence of meshes  $\mathcal{W}_h$ .

We notice that the theoretical predictions of Section 5.2 and Theorem 5.3 are confirmed for all the adopted meshes (noticed that the eigenfunctions are analytical).

*Test 6.2.* We consider the same eigenvalue problem of Test 6.1 and we study the performance of the VEM discretization by comparing the non stabilized virtual method (14) with the stabilized one (17).

We use the polygonal decompositions listed above and polynomial degree of accuracy  $k = 1$ . In Table 1, 2, 3, 4 we show respectively the results for the sequences of meshes  $\mathcal{V}_h$ ,  $\mathcal{T}_h$ ,  $\mathcal{Q}_h$  and  $\mathcal{W}_h$ .

	h	$\lambda_1 = 2\pi^2$	$\lambda_2 = 5\pi^2$	$\lambda_4 = 8\pi^2$	$\lambda_5 = 10\pi^2$
stab	1/8	$1.5116592e-2$	$3.1853832e-2$	$5.8016345e-2$	$6.6969979e-2$
	1/16	$3.6789314e-3$	$8.0145661e-3$	$1.4210222e-2$	$1.8801990e-2$
	1/32	$7.0012743e-4$	$1.7301102e-3$	$3.3396963e-3$	$4.7777198e-3$
	1/64	$3.0444324e-4$	$5.2108531e-4$	$8.3670719e-4$	$1.2482780e-3$
non stab	1/8	$1.6259982e-2$	$3.4992137e-2$	$6.5206325e-2$	$7.1066444e-2$
	1/16	$3.7077944e-3$	$8.3763470e-3$	$1.4886894e-2$	$1.6482121e-2$
	1/32	$9.0559456e-4$	$2.1980346e-3$	$3.5765138e-3$	$4.2714819e-3$
	1/64	$2.2282335e-4$	$5.4246006e-4$	$8.9030896e-4$	$1.0970894e-3$

Table 1: Test 2.  $\epsilon_{h,\lambda}$  for the sequence of meshes  $\mathcal{V}_h$  with  $k = 1$  using stabilized and non stabilized bilinear form (cf. (17) and (14)).

We can observe that the results in the tables confirm the theoretical rates of convergence stated in Section 5.1 and 5.2. Moreover, we observe that the stabilized method exhibit smaller errors than the non stabilized method, at least for this example and with the adopted meshes.

Finally we test the robustness of the method with respect to the stabilization parameter  $\tau_P$  in (16). In Figure 6 we plot the first four eigenvalues obtained by using the method (17) with

	h	$\lambda_1 = 2\pi^2$	$\lambda_2 = 5\pi^2$	$\lambda_4 = 8\pi^2$	$\lambda_5 = 10\pi^2$
stab	1/4	$3.7956531e-2$	$8.2563231e-2$	$1.3775230e-1$	$1.7499322e-1$
	1/8	$9.3559177e-3$	$2.2225550e-2$	$3.8320372e-2$	$4.7423910e-2$
	1/16	$2.8968928e-3$	$5.3035722e-3$	$9.3546517e-3$	$1.1686132e-2$
	1/32	$4.6020029e-4$	$1.1489639e-3$	$2.5315561e-3$	$2.8085686e-3$
non stab	1/4	$3.6516555e-2$	$8.3690017e-2$	$1.3973440e-1$	$1.7640116e-1$
	1/8	$9.7935072e-3$	$2.3455810e-2$	$3.8945871e-2$	$4.7004969e-2$
	1/16	$2.3022736e-3$	$5.7609232e-3$	$9.4339361e-3$	$1.1528350e-2$
	1/32	$5.8111100e-4$	$1.443629e-3$	$2.3277721e-3$	$2.8632288e-3$

Table 2: Test 2.  $\epsilon_{h,\lambda}$  for the sequence of meshes  $\mathcal{T}_h$  with  $k = 1$  using stabilized and non stabilized bilinear form (cf. (17) and (14)).

	h	$\lambda_1 = 2\pi^2$	$\lambda_2 = 5\pi^2$	$\lambda_4 = 8\pi^2$	$\lambda_5 = 10\pi^2$
stab	1/8	$1.8818098e-2$	$5.2487284e-2$	$6.8346353e-2$	$1.1492206e-1$
	1/16	$4.7918544e-3$	$1.3417919e-2$	$1.8818098e-2$	$2.9225446e-2$
	1/32	$1.2031013e-3$	$3.3689281e-3$	$4.7918544e-3$	$7.3099455e-3$
	1/64	$3.0109148e-4$	$8.4307448e-4$	$1.2031013e-3$	$1.8273391e-3$
non stab	1/8	$1.9681403e-2$	$5.6195617e-2$	$8.4024791e-2$	$1.2433816e-1$
	1/16	$4.8440456e-3$	$1.3630519e-2$	$1.9681403e-2$	$2.9719110e-2$
	1/32	$1.2063360e-3$	$3.3819260e-3$	$4.8440456e-3$	$7.3394237e-3$
	1/64	$3.0129322e-4$	$8.4388237e-4$	$1.2063359e-3$	$1.8291604e-3$

Table 3: Test 2.  $\epsilon_{h,\lambda}$  for the sequence of meshes  $\mathcal{Q}_h$  with  $k = 1$  using stabilized and non stabilized bilinear form (cf. (17) and (14)).

	h	$\lambda_1 = 2\pi^2$	$\lambda_2 = 5\pi^2$	$\lambda_4 = 8\pi^2$	$\lambda_5 = 10\pi^2$
stab	1/8	$9.1286449e-2$	$1.6660881e-1$	$1.8692721e-1$	$1.4812532e-1$
	1/16	$1.9606314e-2$	$4.6914763e-2$	$7.6922840e-2$	$9.1770566e-2$
	1/32	$5.5553128e-3$	$1.2633281e-2$	$2.1483001e-2$	$2.6518770e-2$
	1/64	$1.3519999e-3$	$2.8414866e-3$	$5.1009245e-3$	$6.1858195e-3$
non stab	1/8	$1.0129727e-1$	$2.1687715e-1$	$3.3092634e-1$	$7.9649674e-1$
	1/16	$2.0213213e-2$	$5.0080004e-2$	$8.3459711e-2$	$1.0774822e-1$
	1/32	$5.3232288e-3$	$1.3164079e-2$	$2.2779087e-2$	$2.7226046e-2$
	1/64	$1.2759507e-3$	$3.1619628e-3$	$5.2781394e-3$	$6.5472039e-3$

Table 4: Test 2.  $\epsilon_{h,\lambda}$  for the sequence of meshes  $\mathcal{W}_h$  with  $k = 1$  using stabilized and non stabilized bilinear form (cf. (17) and (14)).

$k = 1$  for the sequence of Voronoi meshes  $\mathcal{V}_h$  in Test 6.1 as a function of stabilization parameter  $\tau_P$ .

We observe that the method is robust with respect the stabilization parameter  $\tau_P$ . For reasonable values of  $\tau_P$  and for small enough values of the mesh size  $h$ , the numerical eigenvalues are not effected by the selection of the stabilization parameter. Moreover, as expected, the “critical parameter”, i.e. the minimum value  $\tau_P$  for which the associated method fails, goes like  $h^{-2}$ .

*Test 6.3.* This test problem, as the following one, is taken from the benchmark singular solution set in [32]. We consider the square domain  $\Omega = [-1, 1]^2$  splitted into two subdomains  $\Omega_\delta$  and  $\Omega_1$  (see the left plot in Figure 7), and we study the eigenvalue problem on the square with Neumann homogeneous boundary conditions and discontinuous diffusivity. In this test we consider the

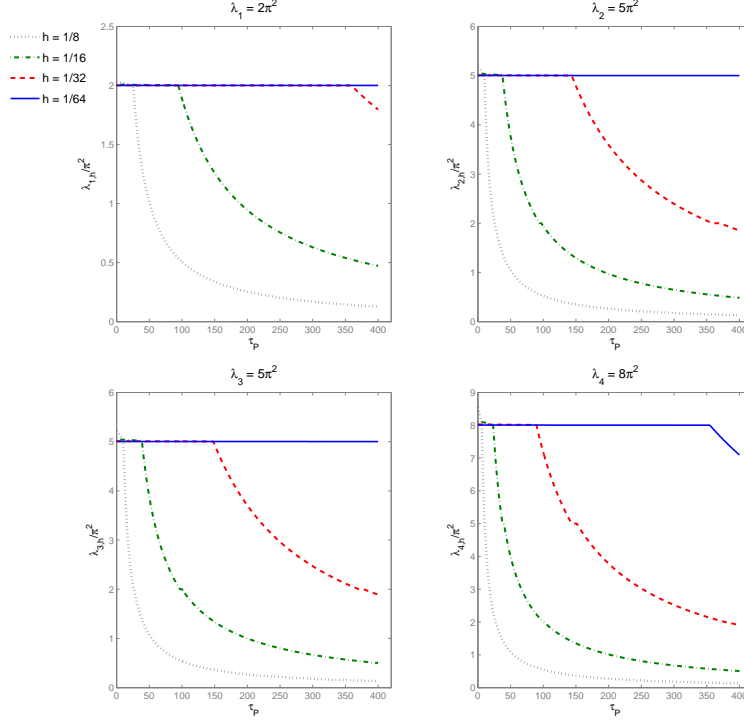


Figure 6: Test 2 .First four eigenvalues as a function of the stabilization parameter  $\tau_P$  (on the abscissas axis).

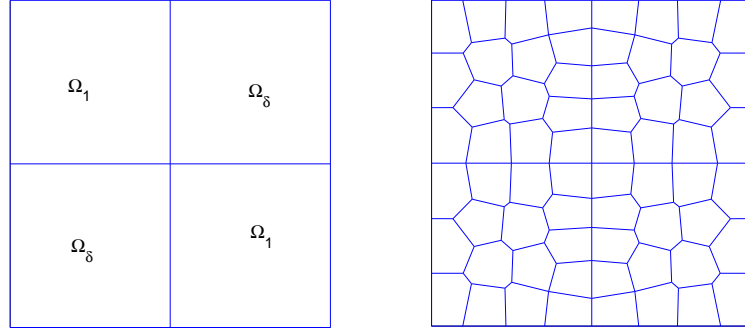


Figure 7: Test 3. Left plot: subdivision of  $\Omega$  into the subdomains  $\Omega_\delta$  and  $\Omega_1$ . Right plot: Example of locally Voronoi decomposition of  $\Omega$ .

continuous bilinear form

$$a_{\mathbb{K}}^P(u, v) := \int_P \mathbb{K} \nabla u \cdot \nabla v \, dx$$

whose virtual approximation (see [12]) is given by

$$a_{h, \mathbb{K}}^P(u_h, v_h) = \int_P \mathbb{K} \Pi_{k-1}^0 \nabla u_h \cdot \Pi_{k-1}^0 \nabla v_h \, dx + \sigma_P S^P \left( (I - \Pi_k^\nabla) u_h, (I - \Pi_k^\nabla) v_h \right) \quad (25)$$

to be used in place of  $a_h^P(u_h, v_h)$  (cf. (10)) in Problem (18). We take  $\mathbb{K}_{|\Omega_1} = I$  and  $\mathbb{K}_{|\Omega_\delta} = \delta I$  with four different values of  $\delta$ , namely  $\delta = 0.50, 0.10, 0.01, 1e-8$ .

We apply the Virtual Element method using a sequence of Voronoi meshes with mesh diameter  $h = 1/2, 1/4, 1/8, 1/16$  (see the right plot in Figure 7 for an example of the adopted

meshes). We show the plot of the convergence for the first and second computed eigenvalues in Figures 8 and 9. We compute the errors  $\epsilon_{h,\lambda}$  by comparing our results with the values given in [32].

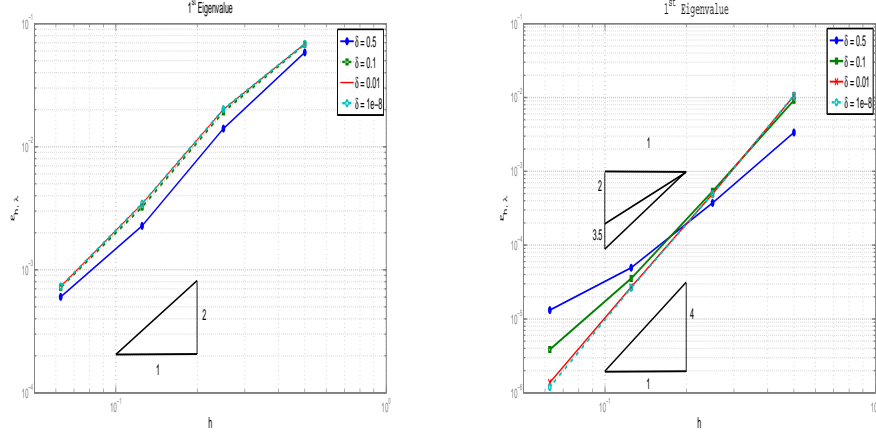


Figure 8: Test 3. Convergence plots for the first eigenvalue and different values of the diffusivity. Left plot:  $k = 1$ . Right plot:  $k = 2$ .

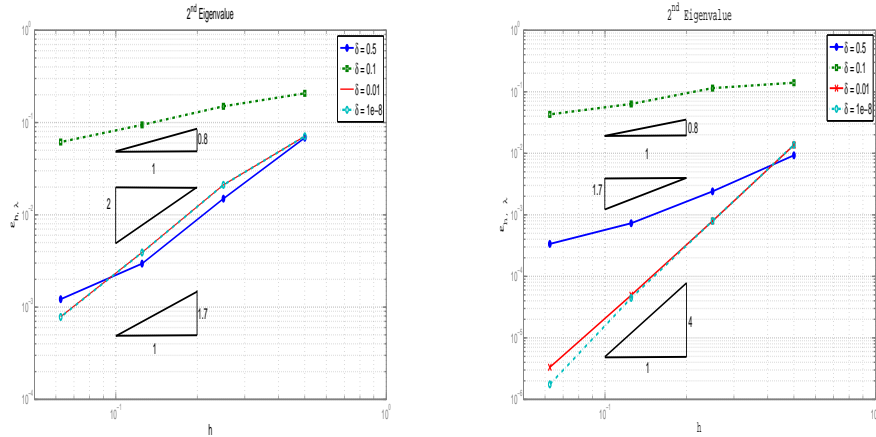


Figure 9: Test 3. Convergence plots for the second eigenvalue and different values of the diffusivity. Left plot:  $k = 1$ . Right plot:  $k = 2$ .

We can observe, in accordance with Theorem 5.3, different rates of convergence that are determined by the polynomial order of the method and by the regularity of the corresponding exact eigenfunctions [32]. Taking this into account, the method is overall optimal, and thus stable with respect to discontinuities in the diffusivity tensor.

*Test 6.4.* In the last test we solve the eigenvalue problem with Neumann boundary conditions on the non-convex L-shaped domain  $\Omega = \Omega_{big} \setminus \Omega_{small}$ , where  $\Omega_{big}$  is the square  $[-1, 1]^2$  and  $\Omega_{small}$  is the square  $[0, 1] \times [-1, 0]$ . Also this test problem is taken from the benchmark singular solution set [32]. We use the sequence of Voronoi decomposition of the domain  $\Omega$  in Figure 10. The convergence results relative to the first and the third eigenvalues are shown in Figure 11. For the first eigenvalue we observe a lower rate of convergence due to the fact that the corresponding eigenfunction is in  $H^{1+r}$ , with  $r = 2/3 - \delta$  for any  $\delta > 0$  (see [32]), while the third eigenfunction is analytical therefore we obtain the optimal order of convergence. The error slopes validate the predicted convergence rates stated in Section 5.2, and confirm the optimality of the method also on non-convex domains.

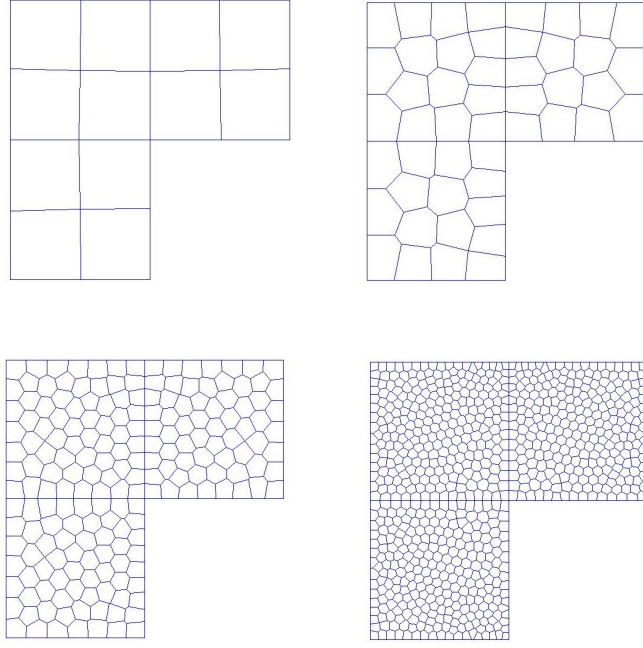


Figure 10: Test 4. Adopted family of meshes for the L-shaped domain  $\Omega$ .

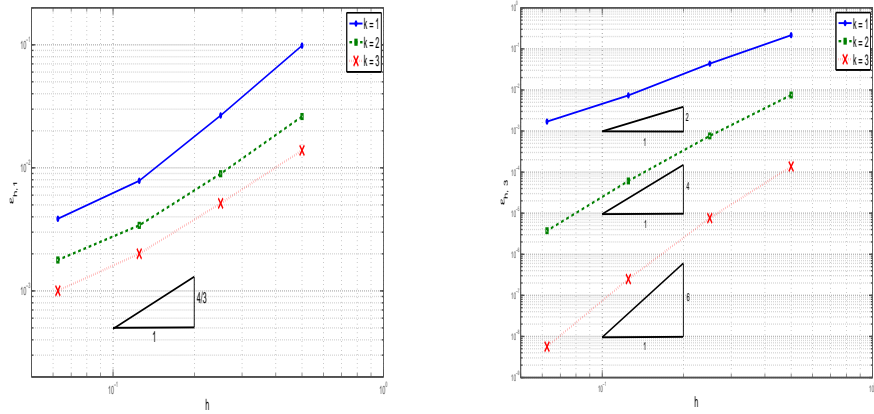


Figure 11: Test 4. Convergence plot for the eigenvalues for the L-shaped domain for the sequence of meshes in Figure 10 and  $k = 1, 2, 3$ . Left plot: first eigenvalue. Right plot: third eigenvalue.

## 7 Conclusions

We have introduced the VEM approximation of elliptic eigenvalue problems. We proved the method is of optimal order both in the approximation of the eigenfunctions and of the eigenvalues. A wide set of numerical test confirm the theoretical results. Further development consists in studying the VEM approximation of eigenvalue problems in mixed form, *a posteriori* error estimates and convergence of adaptive VEM for eigenvalue problems.

## References

- [1] S. Agmon. *Lectures on elliptic boundary value problems*. Prepared for publication by B. Frank Jones, Jr. with the assistance of George W. Batten, Jr. Van Nostrand Mathematical



Studies, No. 2. D. Van Nostrand Co., Inc., Princeton, N.J.-Toronto-London, 1965.

- [2] B. Ahmad, A. Alsaedi, F. Brezzi, L. D. Marini, and A. Russo. Equivalent projectors for virtual element methods. *Comput. Math. Appl.*, 66(3):376–391, 2013.
- [3] P. F. Antonietti, L. Beirão da Veiga, D. Mora, and M. Verani. A stream virtual element formulation of the Stokes problem on polygonal meshes. *SIAM J. Numer. Anal.*, 52(1):386–404, 2014.
- [4] P. F. Antonietti, L. Beirão Da Veiga, S. Scacchi, and M. Verani. A  $C^1$  Virtual Element method for the Cahn-Hilliard equation with polygonal meshes. *SIAM J. Numer. Anal.*, 54(1):34–56, 2016.
- [5] B. Ayuso de Dios, K. Lipnikov, and G. Manzini. The nonconforming virtual element method. *ESAIM Math. Model. Numer. Anal.*, 50(3), 2016.
- [6] I. Babuška and J. Osborn. Eigenvalue problems. In *Handbook of numerical analysis, Vol. II*, Handb. Numer. Anal., II, pages 641–787. North-Holland, Amsterdam, 1991.
- [7] L. Beirão da Veiga, F. Brezzi, A. Cangiani, G. Manzini, L. D. Marini, and A. Russo. Basic principles of virtual element methods. *Math. Models Methods Appl. Sci.*, 23(1):199–214, 2013.
- [8] L. Beirão da Veiga, F. Brezzi, and L. D. Marini. Virtual elements for linear elasticity problems. *SIAM J. Numer. Anal.*, 51(2):794–812, 2013.
- [9] L. Beirão da Veiga, F. Brezzi, L. D. Marini, and A. Russo. The hitchhiker’s guide to the virtual element method. *Math. Models Methods Appl. Sci.*, 24(8):1541–1573, 2014.
- [10] L. Beirão Da Veiga, F. Brezzi, L. D. Marini, and A. Russo. Mixed Virtual Element Methods for general second order elliptic problems on polygonal meshes. *ESAIM Math. Model. Numer. Anal.*, 50(3):727–747, 2016.
- [11] L. Beirão Da Veiga, F. Brezzi, L. D. Marini, and A. Russo. Serendipity face and edge vem spaces. *arXiv preprint arXiv:1606.01048*, 2016.
- [12] L. Beirão da Veiga, F. Brezzi, L. D. Marini, and A. Russo. Virtual Element Method for general second-order elliptic problems on polygonal meshes. *Math. Models Methods Appl. Sci.*, 26(4):729–750, 2016.
- [13] L. Beirão Da Veiga, F. Brezzi, L. D. Marini, and A. Russo. Serendipity Nodal VEM spaces. *Computers & Fluids*, <http://dx.doi.org/10.1016/j.compfluid.2016.02.015>, 2016.
- [14] L. Beirão Da Veiga, F. Brezzi, L.D. Marini, and A. Russo.  $H(\text{div})$  and  $H(\text{curl})$ -conforming VEM. *Numer. Math.*, pages 1–30, 2015.
- [15] L. Beirão da Veiga, A. Chernov, L. Mascotto, and A. Russo. Basic principles of  $hp$  virtual elements on quasiuniform meshes. *Math. Models Methods Appl. Sci.*, 26(8):1567–1598, 2016.
- [16] L. Beirão da Veiga, C. Lovadina, and D. Mora. A Virtual Element Method for elastic and inelastic problems on polytope meshes. *Comput. Methods Appl. Mech. Engrg.*, 295:327–346, 2015.
- [17] L. Beirão da Veiga, C. Lovadina, and A. Russo. Stability analysis for the virtual element method. *arXiv preprint arXiv:1607.05988*, 2016.
- [18] L. Beirão Da Veiga, C. Lovadina, and G. Vacca. Divergence free virtual elements for the Stokes problem on polygonal meshes. *ESAIM Math. Model. Numer. Anal.*, <http://dx.doi.org/10.1051/m2an/2016032>, 2016.
- [19] L. Beirão da Veiga and G. Manzini. A virtual element method with arbitrary regularity. *IMA J. Numer. Anal.*, 34(2):759–781, 2014.

- [20] L. Beirão da Veiga and G. Manzini. Residual *a posteriori* error estimation for the virtual element method for elliptic problems. *ESAIM Math. Model. Numer. Anal.*, 49(2):577–599, 2015.
- [21] M. F. Benedetto, S. Berrone, A. Borio, S. Pieraccini, and S. Scialò. A hybrid mortar virtual element method for discrete fracture network simulations. *J. Comput. Phys.*, 306:148–166, 2016.
- [22] M. F. Benedetto, S. Berrone, S. Pieraccini, and S. Scialò. The virtual element method for discrete fracture network simulations. *Comput. Methods Appl. Mech. Engrg.*, 280:135–156, 2014.
- [23] D. Boffi. Finite element approximation of eigenvalue problems. *Acta Numer.*, 19:1–120, 2010.
- [24] D. Boffi, F. Brezzi, and L. Gastaldi. On the problem of spurious eigenvalues in the approximation of linear elliptic problems in mixed form. *Math. Comp.*, 69(229):121–140, 2000.
- [25] S. C. Brenner and L. R. Scott. *The mathematical theory of finite element methods*, volume 15 of *Texts in Applied Mathematics*. Springer, New York, third edition, 2008.
- [26] F. Brezzi, Richard S. Falk, and L. D. Marini. Basic principles of mixed virtual element methods. *ESAIM Math. Model. Numer. Anal.*, 48(4):1227–1240, 2014.
- [27] F. Brezzi and L. D. Marini. Virtual element methods for plate bending problems. *Comput. Methods Appl. Mech. Engrg.*, 253:455–462, 2013.
- [28] A. Cangiani, E. H. Georgoulis, T. Pryer, and O. J. Sutton. A posteriori error estimates for the virtual element method. *arXiv preprint arXiv:1603.05855*, 2016.
- [29] A. Cangiani, T. Georgoulis, H.M. G. and Pryer, and O. J. Sutton. Conforming and nonconforming virtual element methods for elliptic problems. *arXiv preprint arXiv:1603.05855*, 2016.
- [30] A. Cangiani, V. Gyrya, and G. Manzini. The non-conforming virtual element method for the stokes equations. *arXiv preprint arXiv:1608.01210*, 2016.
- [31] A. Cangiani, G. Manzini, and O. J. Sutton. Conforming and nonconforming virtual element methods for elliptic problems. *arXiv preprint arXiv:1507.03543*, 2015.
- [32] M. Dauge. Benchmark computations for maxwell equations for the approximation of highly singular solutions. URL <http://perso.univ-rennes1.fr/monique.dauge/benchmax.html>, 2004.
- [33] J. Descloux, N. Nassif, and J. Rappaz. On spectral approximation. I. The problem of convergence. *RAIRO Anal. Numér.*, 12(2):97–112, iii, 1978.
- [34] J. Descloux, N. Nassif, and J. Rappaz. On spectral approximation. II. Error estimates for the Galerkin method. *RAIRO Anal. Numér.*, 12(2):113–119, iii, 1978.
- [35] A. L. Gain, C. Talischi, and G. H. Paulino. On the virtual element method for three-dimensional linear elasticity problems on arbitrary polyhedral meshes. *Comput. Methods Appl. Mech. Engrg.*, 282:132–160, 2014.
- [36] T. Kato. *Perturbation theory for linear operators*. Springer-Verlag, Berlin, second edition, 1976.
- [37] D. Mora, G. Rivera, and R. Rodríguez. A posteriori error estimates for a virtual elements method for the steklov eigenvalue problem. *arXiv preprint arXiv: 1609.07154*, 2016.
- [38] D. Mora, G. Rivera, and R. Rodríguez. A virtual element method for the steklov eigenvalue problem. *Math. Models Methods Appl. Sci.*, 25(08):1421–1445, 2015.

- [39] I. Perugia, P. Pietra, and A. Russo. A Plane Wave Virtual Element Method for the Helmholtz Problem. *ESAIM Math. Model. Numer. Anal.*, 50(3):783–808, 2016.
- [40] C. Talischi, G. H. Paulino, A. Pereira, and I. F.M . Menezes. Polymesher: a general-purpose mesh generator for polygonal elements written in matlab. *Struct. Multidisc Optimiz.*, 45(3):309–328, 2012.
- [41] G. Vacca. Virtual element methods for hyperbolic problems on polygonal meshes. *Comput. Math. Appl.*, <http://dx.doi.org/10.1016/j.camwa.2016.04.029>, 2016.
- [42] G. Vacca and L. Beirão Da Veiga. Virtual element methods for parabolic problems on polygonal meshes. *Numer. Methods Partial Differential Equations*, 31(6):2110–2134, 2015.